Probing 2-dimensional protein–protein interactions on model membranes

Martynas Gavutis, Suman Lata & Jacob Piehler

Institute of Biochemistry, Biocenter N210, Johann Wolfgang Goethe-University, Max-von-Laue Straße 9, 60438 Frankfurt am Main, Germany. Correspondence should be addressed to J.P. (j.piehler@em.uni-frankfurt.de)

Published online 7 December 2006; doi:10.1038/nprot.2006.270

This protocol describes an *in vitro* approach for measuring the kinetics and affinities of interactions between membrane-anchored proteins. This method is particularly established for dissecting the interaction dynamics of cytokines with their receptor subunits. For this purpose, the receptor subunits are tethered in an orientated manner onto solid-supported lipid bilayers by using multivalent chelator lipids. Interaction between the ligand with the receptor subunits was probed by a combination of surface-sensitive spectroscopic detection techniques. Label-free detection by reflectance interferometry is used for following assembly of the membrane and tethering of the receptor subunits in quantitative terms. Total internal reflection spectroscopy is used for monitoring ligand binding to the membrane-anchored receptor, for monitoring ligand-receptor interactions by FRET and for monitoring ligand-exchange kinetics. These assays can be used for determining the affinities and stabilities of ligand-receptor complexes in plane of the membrane. The techniques described in this protocol can be established in 2–3 months.

INTRODUCTION

Interactions between proteins anchored or embedded into cellular membranes have an important role for transmembrane signaling. These lateral interactions are not static and are typically triggered or stabilized by further interaction partners such as ligands, effectors and binding proteins from the matrices adjacent to the lipid bilayers. Protein–protein interactions in solution and on the membrane can be described using the same set of differential equations. For several reasons, however, the rate and affinity constants of 2-dimensional interactions cannot be readily deduced from the rate constants of the same interaction in solution: (i) membrane anchoring of proteins reduces their translational and rotational freedom, and results in a preferred orientation of the interaction partners to each other along the normal of the surface. Therefore, the reaction diagram and the reaction coordinate of the interaction are different from the interaction in solution; and (ii) lateral and rotational diffusion of the membrane-anchored protein is much slower than in solution, whereas the dynamics of the amino-acid side chains that mediate the interaction between the proteins are not affected.

Whereas numerous routine techniques for monitoring protein–protein interactions in solution are established, quantitative study of the interactions between membrane-anchored proteins remains challenging. The most crucial issue is to control, quickly change and quantify the concentrations of proteins on the membrane — which is conveniently achievable for proteins in solution. Furthermore, spectroscopic means and suitable assays are required for monitoring 2-dimensional interactions in real time. Label-free techniques for monitoring protein binding to surfaces in real time have proven powerful tools for kinetic characterizations of protein–protein interactions at interfaces. Both optical and acoustic interrogation approaches have proved capable for monitoring mass deposition of a few pg mm^{-2} in real time[1,2]. Optical techniques such as surface plasmon resonance (SPR)[3] or frustrated total internal reflection (resonant mirror)[4] probe the change in refractive index upon protein binding by the evanescent field of a total internally reflected light beam. Reflectance interferometry (RIf)[5] and ellipsometry probe binding to surfaces by directional reflection. Other optical techniques, such as plasmon waveguide resonance spectroscopy[6], can provide more detailed information about the adsorbed adlayer. Acoustic techniques, such as the quartz crystal microbalance (QCM) or surface acoustic waves (SAW), directly sense the mass of the adsorbed proteins, which typically includes the water shell bound to the biomolecules[7]. Furthermore, the changes of the viscoelastic properties of the attached layers can be detected by monitoring energy dissipation (QCM-D)[8]. In combination with optical techniques such as SPR, QCM-D has been used to study the changes in morphology and hydration of surface layers, enabling detection and monitoring conformational changes during ligand binding[9]. Although label-free detection techniques are powerful tools for monitoring and absolutely quantifying surface-mass deposition in real time, they cannot discriminate between different types of molecules, nor provide direct information on interactions in plane of the transducer surface. These limitations are overcome by combination with surface-sensitive fluorescence detection using evanescent field excitation (total internal reflection fluorescence spectroscopy; TIRFS).

In this protocol, we summarize an experimental approach for the quantitative determination of rate and affinity constants of 2-dimensional interactions between membrane-anchored proteins using fluid membranes fused on a glass substrate. A lipid-like molecule carrying a multivalent chelator head group[10] (bis-nitrilotriacetic acid lipid, called bis-NTA lipid in the following) is used for site-specific, orientated tethering of soluble proteins through a histidine-tag onto the membrane in a stable, yet reversible manner (**Fig. 1**). Therefore, the surface concentration of the protein can be flexibly controlled and rapidly changed. This approach was combined with surface sensitive detection techniques, namely RIf and TIRFS[11]. Central to this approach are glass-type substrates for their compatibility with: (i) spontaneous vesicle fusion for assembling solid-supported membranes with high fluidity; (ii) RIF; and (iii) fluorescence excitation and detection in the optical region.

Label-free detection by RIf provides a quantitative monitor of all processes on the surface — including the surface concentrations of the proteins tethered to the membranes. Ligand binding and 2-dimensional interactions can be measured with high sensitivity and versatility by TIRFS. Both the signals are acquired simultaneously, in real time without any crosstalk between them.

Because both techniques are readily used and combined, we describe our set-up in more detail. However, other label-free detection techniques, which might already be established in the investigating laboratory, could be used. Therefore, combination of TIRFS with SPR has already been shown to be feasible[12,13].

Once established, the methodology presented in this protocol enables detailed studies of protein–protein interactions at membranes, and offers versatile application. It is suitable for mimicking the interactions between membrane-tethered proteins, such as interactions mediated by the soluble domains outside the membrane. For transmembrane proteins, polymer-supported membranes have to be used for protein reconstitution on the surface, because the soluble domains tend to stick to the unmodified glass surface. The spectroscopic approach is only suitable for laterally homogeneous membranes: imaging techniques have to be used for studying the effect of microstructured membranes on protein–protein interactions. Artificial membranes are powerful tools for exploring the biophysical principles underlying protein function in membranes under highly controlled conditions, but cannot mimic the complex environment of a protein in a cellular membrane. Understanding of membrane protein function in the cellular context requires techniques that are capable of directly following these processes in the cell. For this purpose, advanced fluorescence imaging techniques including single molecule detection seem most promising, but require demanding technological effort.

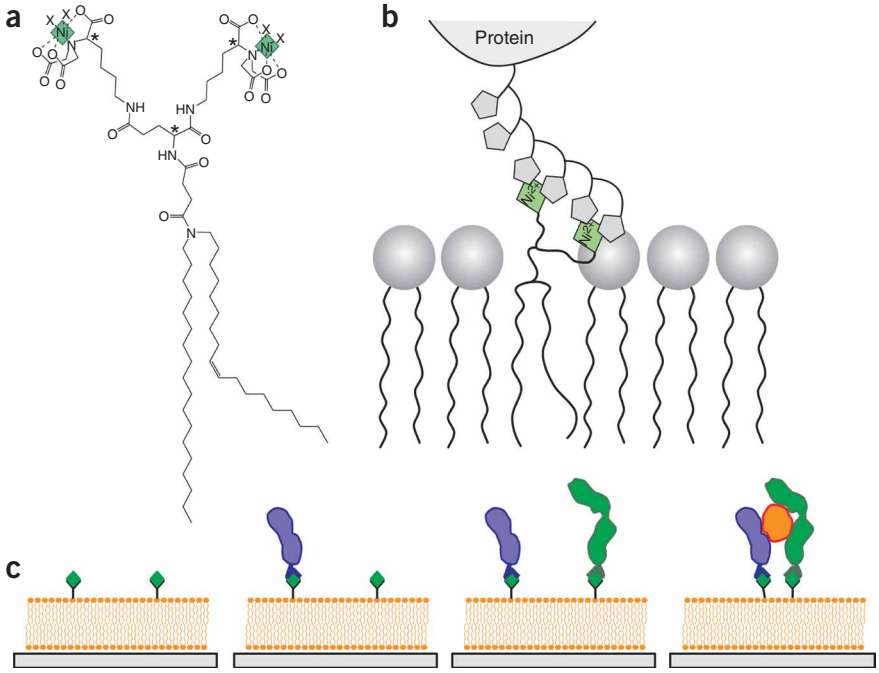

Figure 1 | Orientated and stable tethering of proteins to membranes. (**a**) Chemical structure of the bis-nitrilotriacetic acid lipid (bis-NTA lipid), which is embedded in a membrane to tether his-tagged proteins (**b**). (**c**) The receptor subunits (blue and green) are tethered to solid-supported membranes containing the bis-NTA lipid, followed by binding of the ligand (orange).

Experimental design

The experimental set-up we have established for simultaneous TIRFS and RIf detection is depicted in **Figure 2a**. The components for this set-up have to be obtained from different manufactures. Some components cannot be readily attached to each other, and a mechanical workshop is required for manufacturing adaptors. One of the key elements of the set-up is the prism with a central bore for the fiber bundle required for RIf and for fluorescence detection (**Fig. 2b**). Spectral separation of the two optical techniques is achieved by implementing single-wavelength RIf detection in the near infrared. Therefore, the full visible region is available for fluorescence detection (**Fig. 2c**). The other crucial issue for this set-up is the sample handling by a flow-through system. Different ways of implementing flow through conditions are possible[5,14]. An automatized sample-handling system is desirable, but highly demanding. We suggest starting with a simple approach by using a peristaltic pump and a manual injection valve (**Fig. 2d**). The connection between the injection valve and the flow cell should be as short as possible in order to minimize dead volumes. We use a flow cell with a volume of ~300 nl and a cross-section of 0.1 μm^2, which can be readily manufactured by a mechanical workshop. The small cross-section is not only important for minimizing sample volumes, but also for optimizing mass transport to the surface, which frequently biases the binding kinetics at surfaces[15–17]. For this cell, flow rates between 1 and 250 $\mu l\ s^{-1}$ are practical. The flow rates for the injection of proteins samples are typically 2–10 $\mu l\ s^{-1}$, requiring sample volumes of 200–500 µl. The protocol for assembling this apparatus is presented in **Box 1**.

In this protocol, we will focus on three types of assays, which were the most useful in studying the 2-dimensional interaction dynamics of ternary cytokine-receptor complexes[11,18–21]. The extracellular domains of the receptor subunits are tethered to the membrane in an orientated, stable yet reversible manner through carboxyl (C)-terminal his-tags. In this type of biological system, soluble ligands bind to two receptor subunits and form a ternary complex, which is stabilized by 2-dimensional ligand-receptor interactions (**Fig. 3a**). Monitoring ligand-dissociation kinetics, ligand-exchange kinetics and ligand-receptor interactions by FRET can be used for directly and indirectly quantifying equilibrium and interaction rate constants of these 2-dimensional interactions.

Ligand-dissociation kinetics. See **Figure 3b**. Monitoring the ligand-dissociation kinetics at different receptor surface

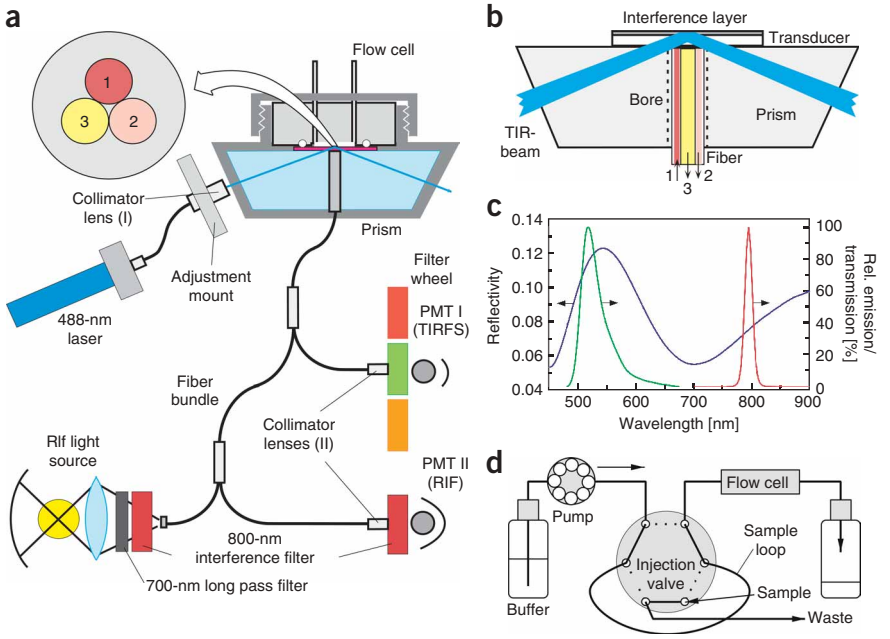

Figure 2 | Experimental set-up for simultaneous total internal reflection fluorescence spectroscopy-reflectance interferometry (TIRFS-RIf) detection. (**a**) Schematic of the set-up. The inset shows a cross-section through the fiber bundle used for RIf (red fibers) and for fluorescence (yellow fiber). (**b**) Enlarged view of the coupling of the light beam for fluorescence excitation into the RIf transducer, and the fibers for RIf illumination (1), RIf detection (2) and fluorescence detection (3). (**c**) Spectral separation of RIf and TIRFS detection: RIf is detected using a filter at 800 nm (dark red curve), leaving the visible range for fluorescence detection. The interference spectrum of the transducer is shown in blue and the emission spectrum of Oregon Green 488 in green (the arrows point to the ordinate relevant for the respective curve). (**d**) Schematic of a simple flow-through system based on a peristaltic pump and an injection valve.

concentrations is a straight-forward assay to probe the mechanism of ternary ligand-receptor complex formation[21]. If carried out with suitable surface concentrations of the receptor subunits, binary and ternary complexes will be in a dynamic equilibrium on the surface. Because ligand dissociation from the binary complex is much faster than from the ternary complex, the equilibrium dissociation constant of 2-dimensional ligand-receptor interactions can be probed by monitoring ligand dissociation. This assay does not necessarily require fluorescence detection, but can be carried out by other label-free detection techniques such as SPR or QCM-D alone. However, low surface concentrations of the receptor subunits and slow dissociation kinetics might require high signal-to-noise ratio and baseline stability, which is unsurpassed for fluorescence detection. Only the ligand needs to be fluorescently labeled for this assay.

Ligand chasing assay. See **Figure 3c**. Chasing labeled ligand in complex with the receptor subunits with an unlabeled ligand is a powerful assay to demonstrate kinetic stabilization of a ternary ligand-receptor complex[21]. This assay is carried out with an excess of one of the receptor subunits tethered to the membrane. After the formation of a ternary complex with a fluorescence-labeled ligand, the excess receptor is loaded with an unlabeled ligand. Owing to

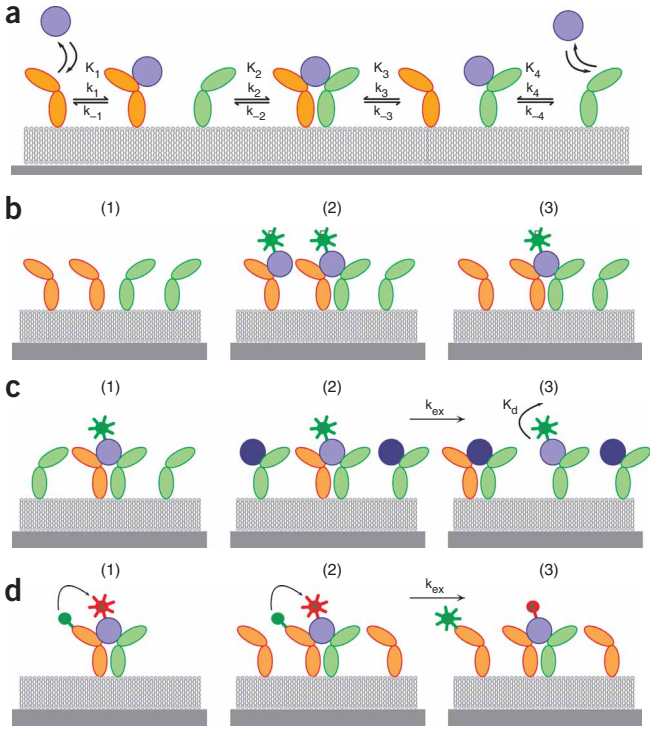

Figure 3 | 2-dimensional dynamics of ternary ligand-receptor complexes. (**a**) The interaction of a ligand (blue) with its two receptor subunits (orange and green) leads to the formation of a ternary ligand-receptor complex through two possible pathways. The population of the pathways depends on the probability of a ligand binding to each of the receptor subunits, therefore, on the rate constants k_1 and k_4, and on the relative surface concentrations of the receptor subunits. (**b**) At surface concentrations in the order of the equilibrium dissociation constant of the 2-dimensional interaction (for example, K_2), an equilibrium between binary and ternary complex is formed. This equilibrium can be monitoring ligand dissociation at different concentrations of the receptor subunits. (**c**) Ligand-chasing assay: ternary complex is formed with an excess of one of the receptor subunits (1). On loading the excess receptor subunit with an unlabeled ligand (dark blue), the labeled ligand is exchanged by 2-dimensional dissociation and association (k_{ex}). If the 2-dimensional dissociation is much slower than ligand dissociation from the surface (k_d), the 2-dimensional dissociation rate constant can be determined from change of surface fluorescence monitored by total internal reflection fluorescence spectroscopy (TIRFS). (**d**) Receptor chasing assay: a ternary complex is formed with fluorescence donor-labeled receptor and acceptor-labeled ligand, leading to FRET. On tethering an excess of unlabeled receptor, the labeled species is exchanged by 2-dimensional kinetics (k_{ex}). By monitoring the decay of the FRET during this process, the 2-dimensional dissociation rate constant of a ligand-receptor interaction can be determined, which is in most cases the rate-limiting step of the exchange process.

BOX 1 | SETUP OF THE DETECTION SYSTEM

(i) Couple the laser beam into the SMA905 terminated 50–100 μm core diameter optical fiber. For efficient coupling, a simple laser-to-fiber coupler (OZ Optics) can be used. An output power of 50–200 μW from the fiber focused onto an area of 2–3 mm^2 is suitable for the excitation of green fluorescent dyes such as Oregon Green 488 or Alexa Fluor 488, and ensures minimum photobleaching.
(ii) Connect the fiber with the adjustable, aberration-corrected, collimator lens (type I) and fix it into the adjustment mount (**Fig. 4**).
(iii) Attach the detection fiber bundle for fluorescence detection as well as for reflectance interferometry (**Fig. 2a,b**). The 600-μm fiber in the center is used for fluorescence detection. Alternatively, a bundle of three or four 600-μm fibers can be used.
(iv) Attach the SMA-terminated fluorescence detection fiber to a collimator lens (type II). Focus through an IR cutting filter and 532 nm or 600 nm interference filter onto the photomultiplier module. Two 15 V DC power supplies have to be combined to provide the photomultiplier module with +15 V and −15 V. These two power supplies can be used to supply all photomultiplier modules in parallel. Connect the signal output of the photomultiplier with the data acquisition card. For most experiments (including FRET), single-color detection is in principle sufficient. For dual-color detection, a filter wheel can be incorporated in order to switch between different colors. Alternatively, a dichroic beam splitter or a fiber bundle with four 600-μm core diameter fibers instead of three can be used in combination with a second photomultiplier.
(v) Connect one of the remaining SMA-terminated branches of the fiber bundle to the tungsten halogen light source. Mount an 800 nm interference filter and a 780-nm long pass filter into the filter slit of the light source. For this purpose, the filter slit has to be extended.
▲ **CRITICAL STEP** Fluorescence and interferometric detection should be spectrally separated to avoid crosstalk between these detection techniques. Fluorophores emitting in a far-red region with an emission maximum >750 nm are not suitable for this set-up.
(vi) Attach the other branch of the SMA terminated fiber bundle to a collimator lens (type II). Focus through an 800 nm interference filter onto the photomultiplier module. Connect the photomultiplier module with the power supplies and the data acquisition card as described above.
(vii) Connect the flow cell with the injection valve and the pump, and connect the outlet of the flow cell with a waste bottle. As a sample loop, connect a 1–2 m long tubing (0.8 mm diameter, therefore 500–1,000 μl volume) with the injection valve.
▲ **CRITICAL STEP** Well-controlled sample handling is crucial for meaningful measurements. We recommend a detailed characterization of the concentration profile in the flow cell during injection of the sample using the background fluorescence during injection of a fluorescence dye[11].
(viii) Mount the transducer into the flow cell with the interference layer pointing to the top and add a drop of refractive index matching oil ($n = 1.52$) between transducer chip and the glass prism. Adjust the focusing lens of the collimator and the adjustment mount to get optimum total internal reflection above the detection fibers.
▲ **CRITICAL STEP** In order to get the highest fluorescence signals and minimum background, the excitation light has to be focused onto the surface of the transducer chip exactly above the detection fiber bundle.
(ix) Sample handling and data acquisition can be readily controlled with software written in LabVIEW (National Instruments). The highest acquisition rate should be used for obtaining the best signal-to-noise ratio. For most binding assays, data averaging over 1 s is suitable. For faster kinetics, data averaging should be adjusted accordingly. The time resolution is limited by the flow system, and rate constants faster than 5 s^{-1} are difficult to resolve by this approach.
(x) For testing of the detection system and the fluidics, as well as for calibration of the RIf signal, small unilaminar vesicles containing fluorescence-labeled lipids should be fused onto the tranducer surface by the same method as described in Steps 1 and 2. For a lipid bilayer, a mass signal of 5 ng mm^{-2} can be assumed. For the transducer and the filters described above, a decrease of 1% in intensity corresponds to an increase in mass loading by 0.7 ng mm^{-2}.

2-dimensional dissociation and re-association, the labeled ligand is exchanged by the unlabeled ligand. If ligand dissociation from the surface is fast, compared with the 2-dimensional dissociation rate constant, the latter can be determined by this assay. With suitable binding affinities of labeled and unlabeled ligand and appropriate receptor surface concentrations, this assay can be used to calculate the 2-dimensional dissociation and association rate constants of ligand–receptor complexes[19]. The most important requirement is to make sure that the 2-dimensional dissociation of the ligand–receptor complex is the rate-limiting step. Again, only the ligand needs to be fluorescently labeled, but an unlabeled ligand with tailored interaction properties is indispensable.

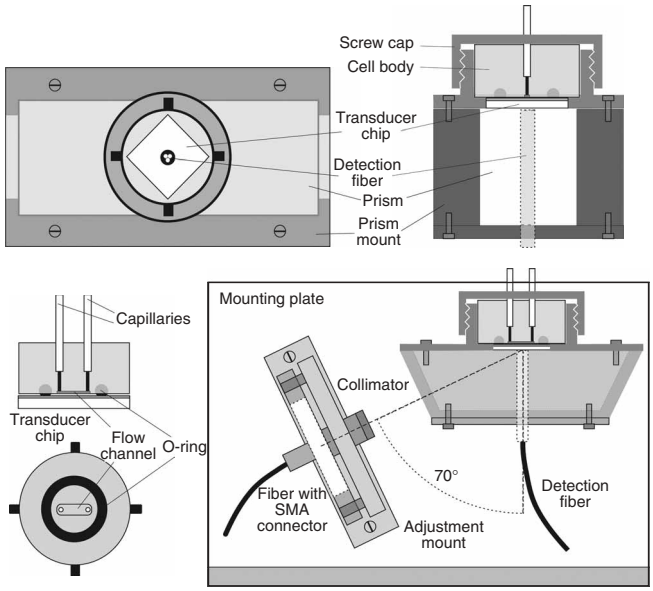

Figure 4 | Detailed drawing of the flow cell and the coupling from the fiber onto the transducer. The prism is fixed into a mount (aluminum), and the flow cell (PVC or POM) is pressed onto the transducer chip from the top. The size of the transducer chip is 12 × 12 mm^2. The flow channel is 3-mm long, 1-mm broad and 100-μm deep, and is connected by stainless steel HPLC capillaries (0.75-mm inner diameter) to the flow system. Both the prism and the adjustment mount are fixed onto a plate providing an angle of incidence of 70°.

Receptor chasing assay. See **Figure 3d**. Monitoring the interaction between the ligand and one of the receptor subunits in the ternary complex by FRET is the most direct way to determine the 2-dimensional dissociation rate constants[18]. This assay makes use of the possibility to rapidly tether competing unlabeled receptor subunits onto the membrane; the formation of a ternary complex with one of the receptor subunits labeled with a fluorescence donor and a ligand labeled with a fluorescence acceptor is detected by FRET. On rapidly tethering an excess (tenfold or more) of unlabeled receptor subunit onto the membrane, the labeled receptor subunit is exchanged by the unlabeled receptor subunit, owing to 2-dimensional dissociation and re-association. Because the association of complexes on the membrane is in most cases fast, the 2-dimensional dissociation kinetics is the rate-limiting step of the exchange[19]. For this assay, site-specific labeling of the ligand and one of the receptor subunits with a fluorescence acceptor and fluorescence donor, respectively, is required.

To do these assays in a meaningful manner, precise control of the surface concentrations of the receptor subunits is crucial. His-tagged protein binds to the Ni (II)-loaded chelator heads on the membrane with concentration-dependent kinetics. Fusion of a tag with 10 histidines was most suitable for stable tethering to bis-NTA lipid. At low surface concentrations (<5 fmol mm^{-2}) and low concentrations of the receptor subunits, the amount of immobilized protein depends linearly on the concentration. However, each protein has its characteristic concentration-dependent binding kinetics. Therefore, scouting experiments are required for each his-tagged protein in order to calibrate surface loading versus receptor concentration.

MATERIALS

REAGENTS

- Purified receptor subunits with a decahistidine-tag (~1 mg)
- Purified receptor subunits without his-tag (~1 mg)
- Purified receptor subunits with a decahistidine-tag, site-specifically labeled with a fluorescence acceptor (yellow-fluorescent dyes such as Alexa Fluor 568 are recommended) (~100 µg) (**Box 2**)
- Purified ligand (~1–2 mg)
- Purified ligand, site-specifically labeled with a fluorescence donor (green-fluorescent dyes such as Oregon Green 488 or Alexa Fluor 488 are recommended; ~500 µg)
- 30% Hydrogen peroxide (medical extra pure, stabilized, Merck KGaA, cat. no. 108597)
- Concentrated sulfuric acid, for analysis (GR for analysis, Merck KGaA, cat. no. 100731)
- Bis-nitrilotriacetic acid (NTA) chelator lipid (synthesis is described in a separate protocol[22]); 1 mM in chloroform
- Synthetic steroyl-oleoyl-phosphatidylcholine (SOPC; Avanti Polar Lipids), 10 mM in chloroform
- Buffer for binding experiments: 20 mM HEPES (pH 7.5) and 150 mM NaCl (Hepes-buffered saline (HBS))
- Nickel (II) chloride, 10 mM in HBS (GR for analysis, Merck KGaA, cat. no. 106717)
- Imidazole, 200 mM in HBS, adjusted to pH 7.5 (ultra, Fluka, cat. no. 56748)
- EDTA, 200 mM in HBS, adjusted to pH 7.5 (analytical grade, Roth, cat. no. 8043.2)

EQUIPMENT

- Probe sonicator, 100–200 W with microtip suitable for volumes of 5–20 ml
- Continuous wave 488-nm argon ion laser with at least 5-mW output power
- 50 or 100 µm optical fiber cord (numerical aperture NA=0.2, 2 m long) with SMA905 connectors (Ocean Optics)
- Bundle of 3 (alternatively 4) optical fibers (600 µm diameter) for fluorescence detection and for Rif, as depicted in the inset of **Figure 2a** (NA=0.4; custom made; Ratioplast-Optoelectronics GmbH)

BOX 2 | FLUORESCENCE LABELING

The assays described in this protocol require fluorescence labeling of the interaction partners. Fluorescence labeling, however, might affect the interaction between the proteins, yet the binding assays require homogeneous binding properties. Furthermore, FRET experiments require a defined labeling degree and position of the fluorophore in the protein. For these reasons, site-specific labeling of the proteins is required, which is typically achieved by thiol-specific reaction (typically with maleimide-functionalized fluorophores) through free cysteine residues incorporated by site-directed mutagenesis. Identifying suitable residues for mutagenesis requires some knowledge of the 3-dimensional structure, because the residue should be exposed and not located in a binding site. In absence of a structure, one possible strategy is to choose an asparagine residue in a potential glycosylation site.

One general problem of cysteine-specific labeling is that many ligands and extracellular receptors domains contain disulfide bridges, which need to be oxidized for appropriate folding. The challenge for cysteine-specific labeling therefore is to maintain the oxidized state of the disulfide bridges while keeping the additional cysteine reduced for labeling. So far we have encountered the following cases and solutions:
(i) Refolding from inclusion bodies solubilized under reducing conditions. Many cytokines can be refolded after complete reduction (preferably in dithiothreitol, DTT) under denaturing conditions. The refolded protein will be oxidized after or during refolding by removing the reducing agent. Subsequently, aggregates should be removed by size exclusion chromatography (SEC), and then the maleimide-functionalized fluorescence dye should be added in a 3-fold molar excess. After reaction overnight at 4 °C in 20 mM Tris-HCl pH 7.5, 150 mM sodium chloride, the labeled protein should be separated from aggregates and excess dye by affinity chromatography or another step of SEC.
(ii) Refolding from inclusion bodies solubilized under non-reducing conditions. In some cases, proteins must not be reduced prior to refolding. In these cases, we observed that the additional cysteine remained in a reduced state. After refolding and removal of aggregates, the protein should be immediately labeled with the maleimide-functionalized fluorescence dye as described above.
(iii) Proteins secreted into the supernatant (for example, insect cell culture). The free cysteine residues of these proteins are typically oxidized, probably by disulfide bonding with sulfhydryl compounds from the medium. These proteins require reduction prior to reaction with the fluorescence dye. Typically, DTT should be incubated at concentrations between 100 µM and 500 µM for 1 h. Subsequently, the reducing agent is removed by SEC, and the protein is reacted with the thiol-rective dye.

In all three cases, it is important to react the protein as soon as possible with the thiol-reactive dye, because the free and exposed sulfhydryl moieties will age (for example, by reacting with each other). In case of reduction prior to the reaction, however, it might be necessary to leave the protein under oxidizing conditions for some time (30–60 min) to allow (re-) formation of internal disulfide bridges. Here, optimization is required in each case.

- Optional: laser-to-fiber coupler (OZ Optics, cat. no. HPUC-25-400/700-M-6AC-2-BL)
- Adjustable, aberration corrected, collimator lens (Optics for Research, cat. no. OFR-CSMA-5-VIS) (collimator type I)
- Adjustable collimator lens (Ocean Optics) (collimator type II)
- Glass prism with a 2.8-mm hole in the center (**Fig. 2b**; custom made, Berliner Glas KGaA)
- 2 (optional 3) photomultiplier modules (Hamamatsu, cat. no. H9307-03)
- 2 power supplies, 15 V DC
- IR cutting filter (Linos Photonics)
- 780-nm long pass filter (LOT Oriel)
- Interference filters: 532 nm, 600 nm and 800 nm (Edmund Optics)
- Optional: motorized filter wheel (CVI Laser Corporation, cat. no. AB-303)
- RIf transducer: 10 nm Ta_2O_5 and 400-nm silica on a 1-mm BK7 glass substrate (custom made, AMP Dünnschichttechnik GmbH). A final size of 12 × 12 mm^2 is required for the flow cell shown in **Figure 4**.
- Tungsten halogen lamp (Ocean Optics, cat. no. HL-2000)
- Prism-mount with flow cell (**Fig. 4**): the prism is attached to a flow cell with a 3-mm long, 1-mm wide and 100-µm deep flow channel (300-nl volume).
- Fluidic system: syringe pump (Microlab 541C), multiple valve positioner (MVP) (both from Hamilton) and autosampler (PS 60; MLE GmbH). Alternatively, a peristaltic pump connected to an injection valve as used for low-pressure liquid chromatography can be used.
- Teflon tubing (0.8-mm inner diameter) and fittings to connect the tubing with the injection valve. Soft silicon tubing is suitable to connect the Teflon tubing to the capillaries of the flow cell.
- Data-acquisition card (PCI-6034E) and LabVIEW programming software (both from National Instruments)
- Software for non-linear curve fitting (for example, Origin from Microcal) and for fitting exponential functions (for example, Berkeley Madonna)

REAGENT SETUP

Preparation of small unilaminar vesicles (SUV) SUVs were prepared by probe sonication. Mix 2.4 µmol SOPC with 0.125 µmol bis-NTA lipid (5 mol%) dissolved in chloroform in a 100 ml round-bottom flask. Evaporate the solvent in a rotary evaporator and re-suspend in 10 ml HBS by swirling and vortexing the round-bottom flask (250 µM final lipid concentration). Probe-sonicate on ice for 10 min with maximum power. Store at 4 °C for short term, or freeze at –20 °C for long term storage. ▲ **CRITICAL** The vesicle suspension should not get hot during probe sonication. The solution should be fully transparent to visual inspection after this treatment. Probe-sonication of the SUV solution should always be done if the solution has been in storage for a few days, or if it has been frozen.

Pretreatment of the transducer surface The silica surface of the transducer has to be cleaned by oxidizing acidic treatment prior to mounting it into the flow chamber. This is achieved by doing the following steps: (1) clean the transducer with water and ethanol and dry them with paper; (2) put them into a clean 100-ml beaker, add 10 ml 30% hydrogen peroxide and then 20-ml concentrated sulfuric acid ! **CAUTION** The hydrogen peroxide – sulfuric acid mixture, also called Piranha solution, is extremely corrosive, wear eye protection. (3) incubate for 30 min and wash extensively with MilliQ water; (4) take out a transducer chip with tweezers and blow dry with nitrogen or argon. Immediately mount the transducer into the flow chamber and start the experiment. ▲ **CRITICAL** After the treatment in step 2 above, the chip should look clean and hydrophilic — the surface remains fully wetted by water after you take it out of the beaker. ▲ **CRITICAL** The cleaned glass surfaces are easily contaminated: do not use transducers if the surface made contact with anything other than clean water or buffer, or if stored after drying for longer than a few minutes. In clean water, the transducer can be stored for a few days.

PROCEDURE

Assembling of solid-supported membranes ● TIMING 10 min

1| Mount a freshly cleaned transducer chip into the flow cell of the detection system and flush the flow cell with running buffer.

2| Inject 250 µM of freshly sonicated SUVs (250 µM lipids) directly onto the silica surface of a freshly cleaned transducer surface for ~100 s, and wash out excess SUVs with running buffer for ~100 s.
▲ **CRITICAL STEP** Bivalent metal ions interfere with fusion of vesicles containing bis-NTA lipids. For this reason we recommend the use of 1 mM EDTA in vesicle suspension.
? TROUBLESHOOTING

3| Inject 10 mM nickel (II) chloride for 40 s followed by 200 mM imidazole for 40 s.
▲ **CRITICAL STEP** This blank immobilization cycle should give a stable baseline in the RIF channel, which should be reached after each regeneration cycle. From now on, any air bubble entering the flow cell will destroy the integrity of the solid-supported membrane. If this happens, the procedure has to be restarted by mounting a new transducer slide (Step 1). A fresh membrane should be prepared for each measurement day.
? TROUBLESHOOTING

Scouting conditions for tethering proteins in controlled concentrations ● TIMING 1 d

4| Inject 10 mM nickel(II) chloride for 40 s followed by injection of the his-tagged receptor subunit (R1) at a concentration of 50 nM for 250 s and rinse for 200 s.
? TROUBLESHOOTING

5| Inject 200 mM imidazole for 40 s to remove the protein.

6| Repeat Steps 4–5 with the other receptor subunit (R2).

7| Determine the molar surface loading obtained in these experiments from the mass-sensitive RIf signal by correcting it with the molar mass of your protein.

Ligand binding to the individual receptor subunits ● TIMING 1 d

8| Inject 10 mM nickel (II) chloride for 40 s followed by injection of the his-tagged receptor subunit (R1) at a concentration of 50 nM for 250 s and rinse for 200 s.

9| Inject the fluorescence-labeled ligand at 100-nM concentration for 150 s and rinse for 100–500 s.
▲ **CRITICAL STEP** Several cytokines show affinity towards transition metal ions, and therefore bind non-specifically to Ni(II)-loaded bis-NTA lipid, which substantially biases the interaction kinetics. Check for such non-specific binding by injecting the ligand without immobilized receptor.

10| If the ligand fully dissociates during rinsing, repeat the injection at various concentrations of the ligand. Otherwise, remove all proteins by injection of 200 mM imidazole for 40 s, and start at Step 8. The concentration range depends on the affinity of the receptor subunits (which can be very different for receptors subunits) and should cover the range from $0.1 \times K_D$ to $10 \times K_D$. In case of low affinity ($k_d > 0.3\ s^{-1}$), the K_D can be determined from the concentration-dependence of the equilibrium response.
? TROUBLESHOOTING

11| Repeat Step 10 with the ligand in complex with the tagless version of the other receptor subunit (R2).
▲ **CRITICAL STEP** These measurements are important for identifying potential cooperativity in the interaction of the ligand with the receptor subunits. For several cytokine receptors, the binding affinity of one of the receptor subunits for the ligand strongly increases on complex formation with the other receptor subunit.

12| Repeat Steps 8–10 with the other receptor subunit.

13| Fit the binding curves using the standard equations for pseudo-first order kinetics (single exponential functions for association and dissociation)[23,24].
▲ **CRITICAL STEP** If the curves are not properly fitted by these functions this might indicate that the kinetics is biased by mass-transport limitations. Another reason for biased kinetics could be non-specific interaction with the surface (Step 9).
? TROUBLESHOOTING

14| The procedures for the ligand dissociation assay (A), the ligand chasing assay (B) and the receptor chasing assay (C) can now be done.

(A) Ligand-dissociation assay ● **TIMING 1 d**

(i) After assembling the membrane on the transducer surface (Step 1–3), inject 10 mM nickel (II) chloride for 40 s followed by sequential injection of the his-tagged receptor subunits R1 and R2 at concentrations suitable to obtain stoichiometric surface loading.

(ii) Inject the fluorescence-labeled ligand for 50–150 s at a concentration sufficient to saturate the binding sites.

(iii) Monitor dissociation for 100–1,000 s.
▲ **CRITICAL STEP** Ternary complex formation is indicated by the fact that ligand dissociation is substantially slower than the dissociation from the individual receptor subunits.
? TROUBLESHOOTING

(iv) Remove all proteins from the lipid-bilayer surface by injection of 200 mM imidazole for 40 s.
▲ **CRITICAL STEP** After imidazole injection, the fluorescence signal should go to the initial baseline. If more than 10–20% of fluorescence signal is left it might be that the lipid bilayer got damaged. In this case we recommend repeating the experiment on a new membrane (Steps 1–3).

(v) Repeat this experiment at 5–10 different concentrations of R1 and R2, but maintain the ratio between R1 and R2.
▲ **CRITICAL STEP** At high receptor-surface concentrations, ligand re-binding can interfere with the dissociation kinetics and complicate data interpretation. If high concentrations are required, re-binding should be eliminated by adding a tagless receptor subunit in the washing buffer. The concentration of the competitor can be determined experimentally or by using the equation described by Goldstein *et al.*[16]

(vi) For data analysis, extract the ligand dissociation curves from the fluorescence channel and set the beginning of the dissociation to zero on the time axis.

(vii) Convert the fluorescence signal into surface concentration (for example, fmol mm^{-2}). At high receptor-surface concentrations, the RIf signal can be used for direct conversion. These signals can be used for calibrating the fluorescence signal, in order to determine the receptor surface concentrations at low concentrations from the ligand binding signal[11].

(viii) Fit the dissociation curves with the differential equations describing the dissociation of the ternary complex. The surface concentrations of the receptor subunits are parameterized as obtained in Step (vii).
▲ **CRITICAL STEP** Fitting of a model requires an understanding of the mechanism of the dissociation process. See ANTICIPATED RESULTS for the differential equations for a 2-step dissociation process, where only one of the two possible pathways (**Fig. 3a**) is taken into account. More details about how these equations were derived, and the differential equations for both association and dissociation pathways can be found in refs. 11,19. However, if the dissociation kinetics does not depend on the surface concentrations of the receptor subunits, fitting this model will not give meaningful results.
? TROUBLESHOOTING

(B) Ligand-chasing assay ● TIMING **1.5 h**

(i) After assembling the membrane on the transducer surface (Steps 1–3), inject 10 mM nickel (II) chloride for 40 s. Sequentially inject R1 and R2 in such concentrations that a tenfold higher surface concentration is obtained for one of the subunits.

(ii) Inject the fluorescence-labeled ligand for 50–150 s at a concentration sufficient to saturate the high-affinity binding sites during the injection.

(iii) Monitor dissociation for 100–1,000 s.

▲ CRITICAL STEP If this experiment is carried out at high surface concentrations of the receptor subunits, tagless receptor might be required in this step in order to minimize re-binding (see ANTICIPATED RESULTS).

(iv) Repeat Step (ii).

(v) During the dissociation phase (100–500 s), inject the unlabeled ligand.

▲ CRITICAL STEP The concentration of the chasing ligand has to be high enough to saturate the binding sites of all excess receptor subunits (10 times above the K_D).

(vi) Remove all proteins from the lipid bilayer surface by injection of 200 mM imidazole for 40 s.

(vii) Fit the fluorescence signal of the spontaneous ligand dissociation kinetics (Step iii) as described in Step A (vi–viii).

(viii) Fit the fluorescence signal of the ligand-dissociation kinetics in presence of unlabeled ligand (Step v) by a mono-exponential decay.

(C) Receptor-chasing assay ● TIMING **1.5 h**

(i) Sequentially inject R1 and fluorescence donor-labeled R2 in such concentrations, that stoichiometric surface loading is obtained.

(ii) Inject the ligand labeled with the FRET acceptor for 50–150 s at a concentration sufficient to saturate the high-affinity binding sites during the injection.

(iii) Monitor spontaneous dissociation for 100–1,000 s.

(iv) Repeat Step 2.

(v) During the dissociation phase (100–1000 s), rapidly tether ~tenfold excess of unlabeled R2 compared with labeled R2 on the membrane. It replaces the labeled R2 in the ternary complex and the FRET signal decays.

(vi) Because the dissociation of R2 is the rate-limiting step during replacement, a mono-exponential fit will give a 2-dimensional dissociation rate constant of R2 leaving the ternary complex.

▲ CRITICAL STEP A mono-exponential fit can be used only if the amount of unlabeled R2 on the membrane is much higher than the amount of unlabeled R2.

(vii) Remove all proteins from the lipid-bilayer surface by injection of 200 mM imidazole for 40 s.

(viii) Repeat Step I–v with unlabeled R2 and direct excitation of the fluorescence label of the ligand.

▲ CRITICAL STEP By this control experiment, ligand dissociation from the surface is determined, which should be negligible. Increase the surface concentrations of the receptor subunits if substantial ligand dissociation is observed.

(ix) For data evaluation, extract the donor and acceptor fluorescence signals after excess R2 was tethered to the membrane (Step v). Invert the donor fluorescence signal by subtracting it from the maximum fluorescence signal (before ligand binding) and subtract the offset (the signal after equilibrium is reached). For the acceptor fluorescence, only the offset signal needs to be subtracted. Fit the curves by a mono-exponential decay. The time constant is the 2-dimensional dissociation rate constant of the interaction of R2 with the complex of the ligand with R1.

● TIMING

Assembling of solid-supported membranes

Steps 1–3, 10 min

Scouting conditions for tethering proteins in controlled concentrations

Steps 4–7, 1 d

Ligand binding to the individual receptor subunits

Steps 8–13, 1 d

Ligand-dissociation assay

Step 14 A, 1 d

Ligand-chasing assay

Step 14 B, 1.5 h

Receptor-chasing assay

Step 14 C, 1.5 h

? TROUBLESHOOTING

Step 2

Frequently, inexperienced users have problems with vesicle fusion. The main cause is either incomplete cleaning of the substrate or contamination of the surface during mounting of the chip. The best read-out for successful cleaning is full wetting of the

surface in clean water. If the water film starts to rupture at the edges of the chip a few seconds after taking it out of the water, it is still not sufficiently clean. Sometimes, a 5 min dip into 3 M sodium hydroxide helps. Also, wiping the surface with paper soaked in ethanol or acetone is helpful. In both cases, subsequent treatment with fresh Piranha is required. Very slow lipid binding indicates that the vesicle suspension might require more sonication. Formation of a lipid bilayer (in contrast to just adsorption of vesicles) is a sharp saturation at a mass signal of $\sim$5 ng mm^{-2}.

Step 3
A fluidic system is prone to generate air bubbles, which inevitably destroy the lipid bilayer. For this reason, degassing of the running buffer is an absolute prerequisite. Furthermore, the temperature of the buffer should not increase during the experiments, as this promotes air-bubble formation. Also, perfusion of the running buffer with Helium or Argon gas reduces the probability for air bubbles.

Step 4
If the his-tagged protein does not bind to the Ni (II)-loaded chelator heads, the sample probably contains too much imidazole or EDTA. We recommend purifying the protein by size exclusion chromatography in the running buffer before use. Unstable tethering of the receptor subunits to the membrane might be observed, in particular if a hexahistidine-tag instead of a decahistidine-tag is used for tethering the receptor subunits. The binding affinity of the tag also substantially affects the concentration-dependent loading of the proteins. For these reasons we recommend always using a decahistidine-tag, because stable tethering of the proteins is a prerequisite for meaningful binding assays. Increased binding stability is also an advantage if low concentrations of imidazole in the background are required to minimize non-specific binding of the ligand (see below).

Step 10
We have observed non-specific binding of several cytokines to the chelated Ni (II) ions on the membrane, which can bias ligand-receptor interactions substantially. If you observe ligand binding in absence of receptor on the membrane, the following strategies are promising: (i) try binding experiments in presence of 5–15 mM imidazole in the background (all buffers). If this works, make sure that the receptor subunits do not dissociate under these conditions. (ii) Block the metal binding sites by tethering an indifferent his-tagged protein. We have successfully used his-tagged maltose binding protein for this purpose. (iii) Identify histidine clusters, which are responsible for transition metal affinity, and mutate key histidine residues.

Step 13
Diffusion of the ligand through the interfacial diffusion layer is a fundamental problem of solid-phase binding assays[15–17]. Most prominent is the non-exponential dissociation kinetics due to rebinding of the ligand after dissociation from one binding site to another. This problem can be overcome by reducing the surface concentration of the tethered receptor (ANTICIPATED RESULTS). In order to test whether the dissociation kinetics is biased by rebinding, unlabeled ligand or the tagless version of the receptor subunit (1 μM) should be injected during the dissociation phase. Under these conditions, rebinding is efficiently suppressed.

Step A (iii)
If the ligand dissociation is not substantially slower with both receptor subunits tethered to the membrane compared to the dissociation from the individual receptor subunits, the ternary complex does not form under these conditions. This might indicate that either the surface concentrations are too low, or that one of the subunits is in excess over the other. Check the activity of the receptor subunits by ligand-binding assays in order to make sure that they are tethered in stoichiometric amounts of active protein on the surface. Increase the surface concentration of the receptor subunits. If the dissociation kinetics is still not mono-exponential, non-specific binding might be involved (see TROUBLESHOOTING Step 4).

Step A (viii)
If the ligand dissociation kinetics does not depend on the surface concentration of the receptor subunits applied in the experiment, it is possible that the applied concentrations are still too high. Therefore, repeat the experiments with drastically reduced surface concentrations of the receptor subunits.

ANTICIPATED RESULTS

Several experimental examples for the interaction assays described above are presented in the following, which were obtained with the type I interferon (IFN) receptor (ifnar). The extracellular domains of the receptor subunits ifnar1 (ifnar1-EC) and ifnar2 (ifnar2-EC) were fused to a decahistidine-tag (ifnar1-H10 and ifnar2-H10, respectively). The ligand IFNα2 and several mutants with altered affinity for the receptor subunits were used. These proteins were site-specifically labeled by incorporating additional cysteine residues. As is typical for cytokine receptors, the ligand is recognized by receptor subunits with different

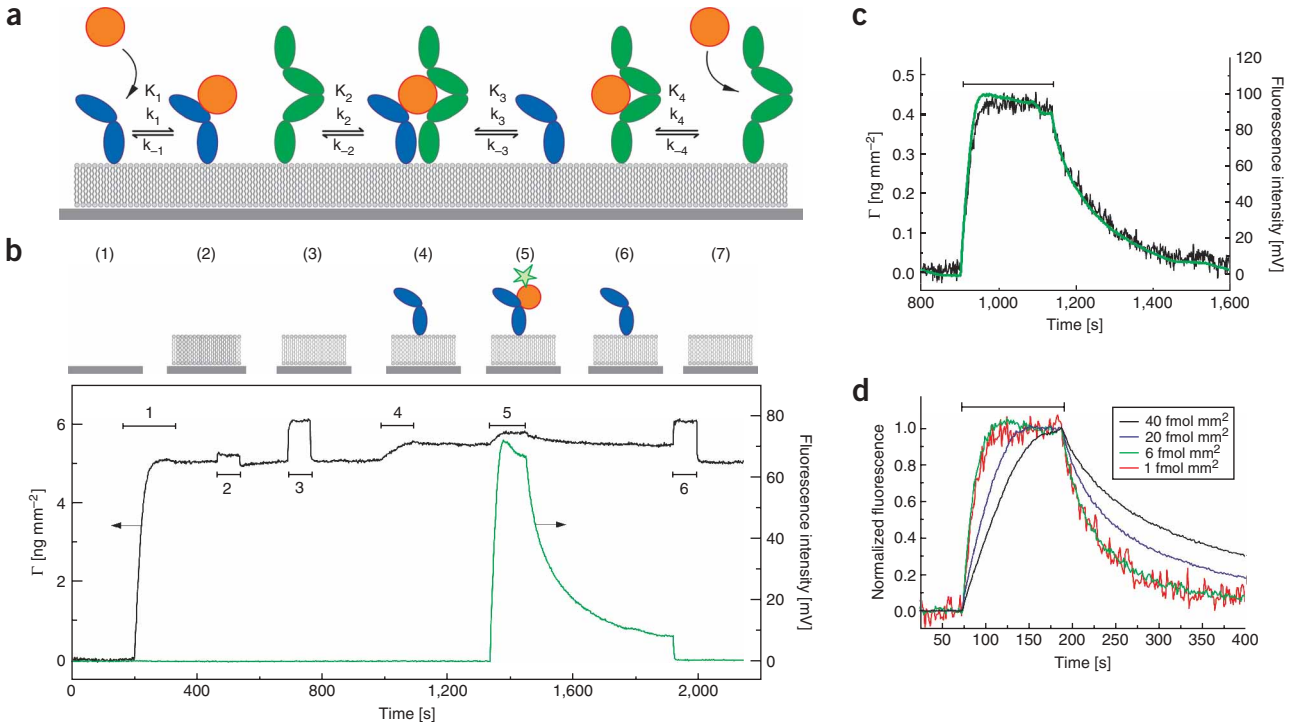

Figure 5 | Membrane assembling, conditioning and binding assay. (**a**) Scheme of the ternary complex formation on interaction if type I interferons (red) with its receptor subunits ifnar2 (blue) and ifnar1 (green). (**b**) Typical sequence of injections for a binding assay as simultaneously detected by reflectance interferometry (Rif; black line) and total internal reflection fluorescence spectroscopy (TIRFS; green line): 1, vesicle fusion; 2, loading with Ni (II) ions; 3, injection of 200 mM imidazole; 4, tethering of ifnar2-H10; 5, binding of fluorescence-labeled IFNα2; 6, regeneration with 200 mM imidazole. (**c**) Overlay of the TIRFS (green line) and RIf (black line) signals during ligand binding and dissociation. (**d**) Ligand binding at different surface concentrations of ifnar2. The binding curves are normalized to the equilibrium-binding signal.

affinities. IFNα2 binds ifnar2-EC with nanomolar affinity, a k_1 of $\sim 3\times10^6$ $M^{-1}s^{-1}$ and a k_{-1} of 0.015 s^{-1}. By contrast, IFNα2 binds ifnar1-EC with micromolar affinity, a k_4 of 2×10^5 $M^{-1}s^{-1}$ and a k_{-4} of ~ 1 s^{-1}.

Lipid bilayer assembling, receptor immobilization and ligand binding assays

A typical experiment showing assembling of the membrane, tethering of ifnar2-EC and its interaction with ^{OG488}IFNα2 as monitored by simultaneous TIRFS-RIf detection is shown in **Figure 5**. Fast vesicle fusion leveling at a mass signal of ~ 5 ng mm^{-2} confirms the formation of a lipid bilayer on the silica surface. In Step 4, ifnar2-H10 was stably tethered to the membrane. All these steps are detected only by RIf. On injection of ^{OG488}IFNα2, corresponding signals are detected on both the RIf and the TIRFS channel. Dissociation of the ligand during buffer wash was monitored for 500 s, followed by removal of all proteins from the membrane by injection of 200 mM imidazole. Overlay of the binding curves detected by the two independent methods (**Fig. 5b**) is recommended in order to make sure that the same process was observed. In **Figure 5c**, binding curves for the interaction of IFNα2 with ifnar2-EC at different surface concentrations are compared by normalizing the binding curves to the equilibrium response. The fact that both association and dissociation get faster with decreasing surface concentration of ifnar2-H10 indicates that these curves are biased by rebinding, which is due to the high k_a of the interaction.
At receptor surface concentrations of 6 fmol mm^{-2} and below, the curvature of the binding curves is independent of the receptor surface concentration (the normalized binding curves overlay), indicating that rebinding is negligible under these conditions.

Ligand dissociation from the ternary complex

Typical binding assays of IFNα2 with both the receptor subunits tethered onto the membrane are shown in **Figure 6a–c**. Ifnar2-H10 and ifnar1-H10 were subsequently tethered either in stoichiometric ratio (**Fig. 6a,b**), or with an excess of ifnar1-H10 (**Fig. 6c**). Subsequently, 100 nM ^{OG488}IFNα2 were injected and binding was monitored in the TIRFS channel. At high concentrations of receptor subunits, very slow dissociation can be observed (**Fig. 6a**), whereas at lower surface concentrations substantially faster dissociation kinetics is observed (**Fig. 6b**). However, stable ligand binding was also observed with low surface concentrations of ifnar2-H10 and high surface concentrations of ifnar1-H10 (**Fig. 6c**). These properties indicate a 2-step

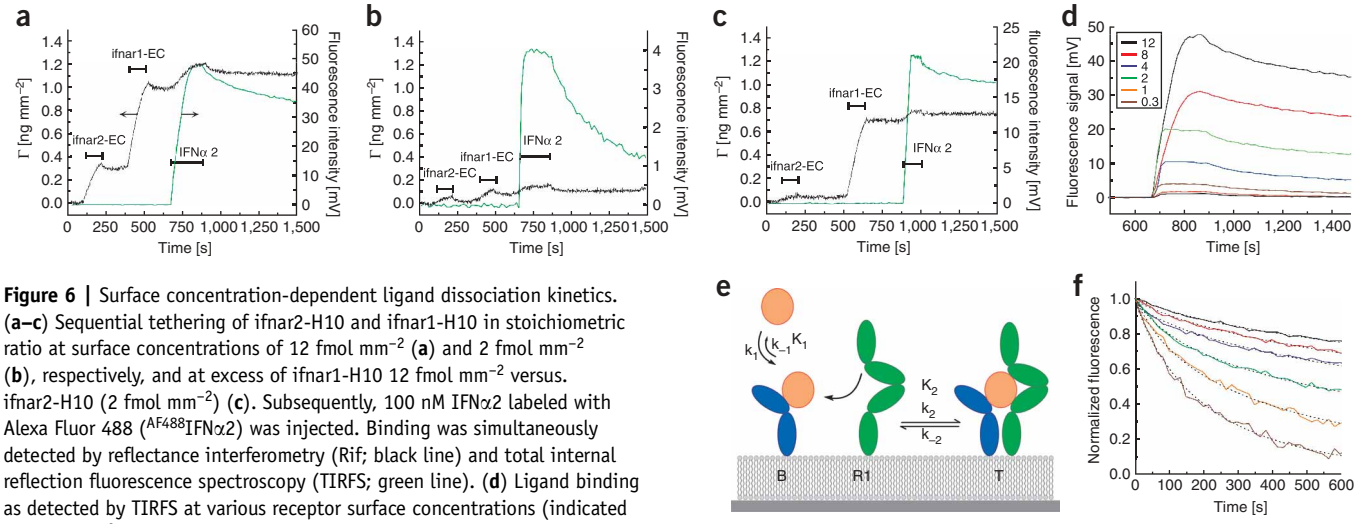

Figure 6 | Surface concentration-dependent ligand dissociation kinetics. (**a–c**) Sequential tethering of ifnar2-H10 and ifnar1-H10 in stoichiometric ratio at surface concentrations of 12 fmol mm^{-2} (**a**) and 2 fmol mm^{-2} (**b**), respectively, and at excess of ifnar1-H10 12 fmol mm^{-2} versus. ifnar2-H10 (2 fmol mm^{-2}) (**c**). Subsequently, 100 nM IFNα2 labeled with Alexa Fluor 488 (^{AF488}IFNα2) was injected. Binding was simultaneously detected by reflectance interferometry (Rif; black line) and total internal reflection fluorescence spectroscopy (TIRFS; green line). (**d**) Ligand binding as detected by TIRFS at various receptor surface concentrations (indicated in fmol mm^{-2} in the legend). (**e**) 2-step assembling model used for fitting the ligand dissociation kinetics where the ligand (orange) binds first to ifnar2-H10 (blue) to form a binary complex (B) and recruits ifnar1-H10 (green, R1) only on membrane into the ternary complex (T). (**f**) Normalized ligand dissociation kinetics at various receptor surface concentrations, and fit of the 2-step dissociation model (dotted lines).

assembling process (**Fig. 3a**). Ligand binding kinetics measured at various receptor surface concentrations are compared in **Figure 6d**. Because association to ifnar2 is faster than to ifnar1, pathway 1 is more likely than pathway 2 (**Fig. 5a**) at stoichiometric amounts of the receptor subunits. If only the dominating pathway (**Fig. 6e**) is taken into account, the ligand dissociation curves can be fitted by the following set of differential equations[11] (**Fig. 6f**):

$$\frac{d[T]}{dt} = k_2 \cdot [B] \cdot ([R1]_0 - [T]) - k_{-2} \cdot [T]$$

$$\frac{d[B2]}{dt} = -k_2 \cdot [B] \cdot ([R1]_0 - [T]) + k_{-2} \cdot [T] - k_{-1} \cdot [B]$$

$$[S] = [T] + [B], \text{ with } T_{t=0} = [R2]_0, [B]_{t=0} = 0$$

The surface concentrations of the receptor subunits $[R1]_0$ and $[R2]_0$ are determined from the RIf signals. The dissociation rate constant of the binary complex k_{-1} is determined from binding assays with ifnar2-H10 tethered to the membrane alone. The 2-dimensional dissociation rate constant of the binary complex k_{-2} is here assumed to be the same as the corresponding

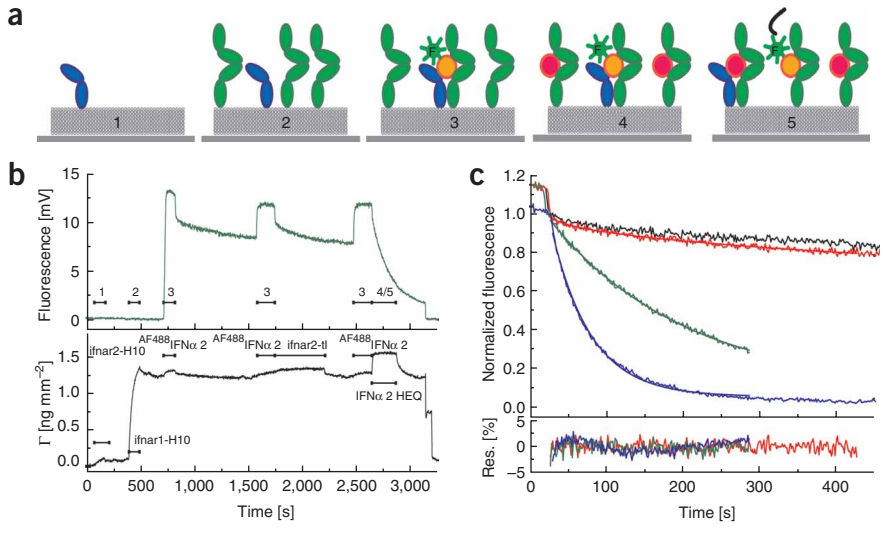

Figure 7 | Ligand chasing assay. (**a**) Schematic of the assay: ternary complex on fluid lipid membrane was formed by sequential injection of ifnar2-H10 (blue) (1), a large excess of ifnar1-H10 (green) (2) and IFNα2 labeled with Alexa Fluor 488 (orange) (^{AF488}IFNα2) (3). The excess of ifnar1 was then loaded with an unlabeled competitor (pink) (4), which binds ifnar1 with high affinity (IFNα2 HEQ) and exchanged the labeled ligand in the ternary complex (5). (**b**) Typical experiment carried out with the wild-type proteins as detected by total internal reflection fluorescence spectroscopy (TIRFS; green) and by reflectance interferometry (Rif; black) (2 fmol mm^{-2} ifnar2-H10, 20 fmol mm^{-2} ifnar1-H10). After the second injection of ^{AF488}IFNα2, 2 μM tagless ifnar2-H10 (ifnar2-tl) was injected to eliminate rebinding. After the third injection of ^{AF488}IFNα2, 1 μM unlabeled IFNα2 HEQ was injected. (**c**) Overlay of the normalized ^{AF488}IFNα2 dissociation curves from (**b**): spontaneous dissociation during washing with buffer (black) and with 2μM ifnar2-tl (red), as well as dissociation while chasing with IFNα2 HEQ (green). Dissociation from ifnar2-H10 alone is shown for comparison (blue). The residuals from the curve fits are shown at the bottom.

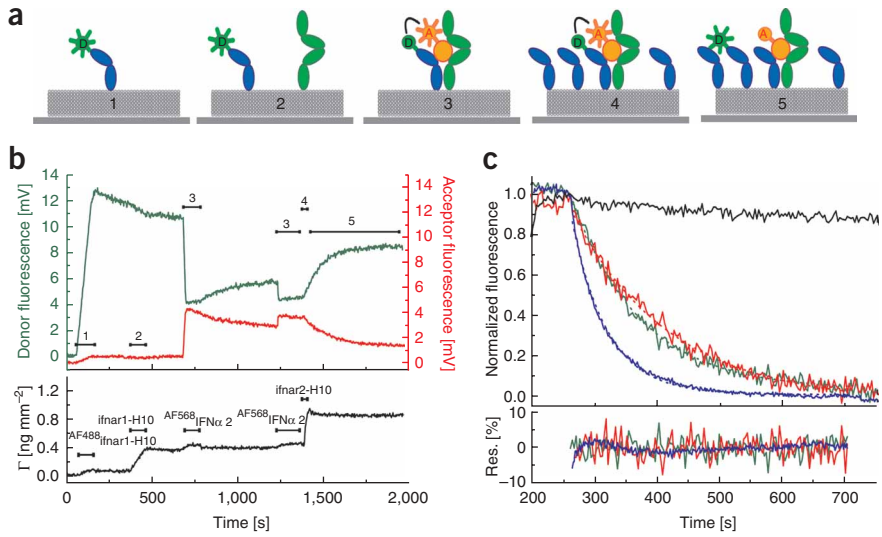

Figure 8 | Receptor chasing assay. (**a**) Principle of surface dissociation rate constant determination as detected by FRET: the ternary complex on the fluid lipid membrane is formed by sequential injection of ifnar2-H10 labeled with Alexa Fluor 488 (^{AF488}ifnar2-H10) (1), ifnar1-H10 (2) and IFNα2 labeled with Alexa Fluor 568 (^{AF568}IFNα2) (3). Equilibrium is then perturbed by rapidly tethering an excess of non-labeled ifnar2-H10 onto the membrane (4), which exchanges the labeled ifnar2-H10 in the ternary complex (5). (**b**) Course of a typical experiment monitoring donor fluorescence (green) and acceptor (red trace) fluorescence by total internal reflection fluorescence spectroscopy (TIRFS) and the mass loading by reflectance interferometry (Rif; black) (2 fmol mm^{-2} ^{AF488}ifnar2-H10, 5 fmol mm^{-2} ifnar1-H10, 16 fmol mm^{-2} ifnar2-H10). (**c**) Comparison of the surface dissociation rates from donor (green) and acceptor (red) channels with the dissociation of ^{AF568}IFNα2 from ifnar2-H10 alone (blue). A control experiment carried out the same way, but with unlabeled ifnar2-H10 in (1) and with direct excitation of ^{AF568}IFNα2 confirmed negligible ligand dissociation from the surface (black). The residuals from mono-exponential curve fits are shown at the bottom.

dissociation rate constant for ligand dissociation into the solution (k_{-4}). The only fitted parameter is the 2-dimensional association rate constant k_2. Since k_2 and k_{-2} are highly correlated, these parameters cannot be simultaneously fitted. The robust parameter, which can be properly determined by this fit is the 2-dimensional equilibrium constant $K_2 = k_2/k_{-2}$. More details about how these equations were derived, and the differential equations for both association and dissociation pathways can be found in references[11,19].

Ligand-chasing assay

An example for the determination of a 2-dimensional dissociation rate constant by a ligand displacement assay (**Fig. 7e**) is shown in **Figure 7b**. High excess of ifnar1-H10 was tethered to the membrane. After binding of fluorescent-labeled IFNα2, an initial fast decay of the fluorescence signal corresponding to ligand that is transiently bound to excess ifnar1-H10 was observed. This was followed by the slow, spontaneous dissociation of the ligand from the ternary complex. The same experiment was repeated with tagless ifnar2-EC in the washing buffer in order to minimize rebinding. After the third injection, an unlabeled IFNα2 mutant with increased affinity to ifnar1 was injected, and the exchange of the labeled ligand in the ternary complex was monitored by TIRFS. Since the dissociation of the labeled ligand from ifnar1 is very fast, the rate-limiting step in this process is the 2-dimensional dissociation of the IFNα2-ifnar2 complex. Strikingly, this dissociation process is ~5-times slower than the dissociation of free IFNα2 from ifnar2-EC (**Fig. 7c**).

Receptor-chasing assay

A typical experiment for measuring 2-dimensional dissociation kinetics by FRET is shown in **Figure 8**. Ifnar2-H10 labeled with fluorescence donor and unlabeled ifnar1-H10 were sequentially tethered onto the membrane. On binding of the ligand labeled with an acceptor dye (Alexa Fluor 568), FRET was detected both on the donor and the acceptor channels (**Fig. 8b**). Slow dissociation of the ligand was observed as expected at these surface concentrations. After a second injection of the ligand, however, the resulting ternary complex was chased by rapidly tethering a large excess of unlabeled ifnar2-H10 onto the membrane. Much faster recovery of the donor fluorescence and similar decay of the sensitized fluorescence was observed. However, this was not due to ligand dissociation, which was hardly detectable under these conditions (**Fig. 8c**), but to the exchange of labeled versus unlabeled ifnar2-EC in the ternary complex. Therefore, the 2-dimensional dissociation kinetics of the ifnar2-H10/IFNα2 interaction as the rate-limiting step of this process was probed. Again, slower dissociation in plane of the membrane was observed, suggesting a more complicated dissociation mechanism.

COMPETING INTERESTS STATEMENT The authors declare that they have no competing financial interests.

Published online at http://www.natureprotocols.com
Reprints and permissions information is available online at http://npg.nature.com/reprintsandpermissions

1. Cooper, M.A. Label-free screening of bio-molecular interactions. *Anal. Bioanal. Chem.* **377**, 834–842 (2003).
2. Homola, J. Present and future of surface plasmon resonance biosensors. *Anal. Bioanal. Chem.* **377**, 528–539 (2003).
3. Liedberg, B., Nylander, C. & Lundstrom, I. Surface-plasmon resonance for gas-detection and biosensing. *Sens. Actuators* **4**, 299–304 (1983).

4. Edwards, P.R. *et al.* Kinetics of protein–protein interactions at the surface of an optical biosensor. *Anal. Biochem.* **231**, 210–217 (1995).
5. Schmitt, H.M., Brecht, A., Piehler, J. & Gauglitz, G. An integrated system for optical biomolecular interaction analysis. *Biosensors & Bioelectronics* **12**, 809–816 (1997).
6. Salamon, Z., Macleod, H.A. & Tollin, G. Coupled plasmon-waveguide resonators: a new spectroscopic tool for probing proteolipid film structure and properties. *Biophys. J.* **73**, 2791–2797 (1997).
7. Marx, K.A. Quartz crystal microbalance: a useful tool for studying thin polymer films and complex biomolecular systems at the solution-surface interface. *Biomacromolecules* **4**, 1099–1120 (2003).
8. Hook, F. *et al.* Variations in coupled water, viscoelastic properties, and film thickness of a Mefp-1 protein film during adsorption and cross-linking: a quartz crystal microbalance with dissipation monitoring, ellipsometry, and surface plasmon resonance study. *Anal. Chem.* **73**, 5796–5804 (2001).
9. Reimhult, E., Larsson, C., Kasemo, B. & Hook, F. Simultaneous surface plasmon resonance and quartz crystal microbalance with dissipation monitoring measurements of biomolecular adsorption events involving structural transformations and variations in coupled water. *Anal. Chem* **76**, 7211–7220 (2004).
10. Lata, S., Reichel, A., Brock, R., Tampé, R. & Piehler, J. High-affinity adaptors for switchable recognition of histidine-tagged proteins. *J. Am. Chem. Soc.* **127**, 10205–10215 (2005).
11. Gavutis, M., Lata, S., Lamken, P., Müller, P. & Piehler, J. Lateral ligand-receptor interactions on membranes probed by simultaneous fluorescence-interference detection. *Biophys. J.* **88**, 4289–4302 (2005).
12. Liebermann, T. & Knoll, W. Surface-plasmon field-enhanced fluorescence spectroscopy. *Colloids and Surfaces a-Physicochemical and Engineering Aspects* **171**, 115–130 (2000).
13. Neumann, T., Johansson, M.L., Kambhampati, D. & Knoll, W. Surface-plasmon fluorescence spectroscopy. *Advanced Functional Materials* **12**, 575–586 (2002).
14. Piehler, J. & Schreiber, G. Fast transient cytokine-receptor interactions monitored in real time by reflectometric interference spectroscopy. *Analytical Biochemistry* **289**, 173–186 (2001).
15. Glaser, R.W. Antigen-antibody binding and mass transport by convection and diffusion to a surface: a two-dimensional computer model of binding and dissociation kinetics. *Anal. Biochem.* **213**, 152–61 (1993).
16. Goldstein, B., Coombs, D., He, X., Pineda, A.R. & Wofsy, C. The influence of transport on the kinetics of binding to surface receptors: application to cells and BIAcore. *J. Mol. Recognit.* **12**, 293–299 (1999).
17. Schuck, P. & Minton, A.P. Analysis of mass transport-limited binding kinetics in evanescent wave biosensors. *Anal. Biochem.* **240**, 262–272 (1996).
18. Lata, S., Gavutis, M. & Piehler, J. Monitoring the dynamics of ligand-receptor complexes on model membranes. *J. Am. Chem. Soc.* **128**, 6–7 (2006).
19. Gavutis, M., Jaks, E., Lamken, P. & Piehler, J. Determination of the 2-dimensional interaction rate constants of a cytokine receptor complex. *Biophys. J.* **90**, 3345–3355 (2006).
20. Lamken, P. *et al.* Functional cartography of the extracellular domain of the type I interferon receptor subunit ifnar1. *J. Mol. Biol.* **350**, 476–88 (2005).
21. Lamken, P., Lata, S., Gavutis, M. & Piehler, J. Ligand-induced assembling of the type I interferon receptor on supported lipid bilayers. *J. Mol. Biol.* **341**, 303–318 (2004).
22. Lata, S. & Piehler, J. A multivalent chelator lipid for stably tethering histidine-tagged proteins onto membranes. *Nature Protocols* (2006)(doi:10.1038/nprot.2006.271).
23. Eddowes, M.J. Direct immunochemical sensing: basic chemical principles and fundamental limitations. *Biosensors* **3**, 1–15 (1987).
24. Karlsson, R., Michaelsson, A. & Mattsson, L. Kinetic analysis of monoclonal antibody-antigen interactions with a new biosensor based analytical system. *J. Immunol. Methods* **145**, 229–240 (1991).